www.czasopisma.pan.pl PAN POLSKA AKADEMIA NAUK www.journals.pan.pl

PAN ARCHIVES OF ACOUSTICS
Vol. **39**, No. 1, pp. 51–63 (2014)

DOI: 10.2478/aoa-2014-0006

A Versatile Model of Nonlinear Electrodynamic Loudspeaker Co-Operating with the Amplifier Designed by Way of Advanced Software

Mehran ERZA[(1)], Etienne GAVIOT[(1)], Guy LEMARQUAND[(1)], Pascal TOURNIER[(2)], Lionel CAMBERLEIN[(1)], Stephane DURAND[(1)], Frederic POLET[(1)]

[(1)] *Laboratoire d'Acoustique de l'Universite du Maine UMR CNRS 6613*
Avenue Olivier Messiaen, 72085 Le Mans Cedex 9, France; e-mail: mehran.erza@yahoo.com, {etienne.gaviot, guy.lemarquand, lionel.camberlein, stephane.durand, frederic.polet}@univ-lemans.fr

[(2)] *ON Semiconducter; FRANCE SAS, 132, Chemin de Basso Cambo, BP53512*
31035 Toulouse Cedex1, France; e-mail: pascal.tournier@onsemi.com

(*received July 2, 2013; accepted January 7, 2014*)

Sound processing with loudspeaker driving depends critically on high quality electroacoustic transducers together with their relevant amplifiers. In this paper, the nonlinear effects of electrodynamic loudspeakers are investigated as regard the influence of the changes of their main descriptive parameters values. Indeed, while being operated nonlinear effects observed with loudspeakers are due to changes of such constitutive parameters. Regarding either current or voltage-drive, an original model based on Simulink® is presented, taking account of all the electrical and mechanical properties closely associated with nonlinear behaviours. Moreover, as such a Simulink® model may be combined with the PSpice® advanced software, the behaviour of both loudspeaker and amplifier can be exhaustively investigated and optimized. To this end, the amplifier is simulated thanks to the Orcad-Capture-PSpice® software prior to match with the loudspeaker model with the so-called SLPS co-simulator. Then, values of the current flowing through the loudspeaker can be determined and plotted considering voltage controlling. Obviously in this case current-drive has not to be assessed.

This way to proceed allows us to highlight any critical information especially due to the voice coil displacement, yielded velocity, and acceleration of the diaphragm. Indeed our approach testifies to the imperative necessity of mechanical measurements together with electrical ones. Then, considering a given amplifier-loudspeaker association with specific parameters changes of the latter, the entailed nonlinear distortion allows us to qualify and criticize the whole design. Such an original approach should be most valuable so as to match the best fitted amplifier with a given electrodynamic loudspeaker. Then non linear effects due to voltage and current-drive are compared highlighting the advantages of an apt current-controled policy.

Keywords: loudspeaker, nonlinear effects, advanced software, current-driving, force factor.

1. Introduction

Classical models for implementing loudspeakers in sundry versatile electronics software are usually quite simple since based on RLC circuits (Vanderkooy, 1989; Wright, 2008; Klippel, 2004; Thorborg *et al.*, 2007). Whatever the version considered in the literature, despite ensuring the impedance *versus* frequency relationship, such models have so far proved unable to account for the numerous shortcomings of loudspeakers, and most especially their nonlinear limitations. Indeed, as neither electromechanical properties nor physical quantities such as displacement, velocity, acceleration and force may be considered, nonlinear behaviours are out of reach of such models.

The main purpose of this paper is to present advanced models of nonlinear loudspeakers so as to access to both their electrical and mechanical properties, with respectively the current and its nonlinear distortion, and the acceleration and relevant distortion as regards either voltage or current-drive of the transducer. To this end, we consider a loudspeaker reference model and its associated parameters as introduced in (Strurtzer *et al.*, 2012) together with the character-

istics of either specific classical amplifier devices, or specificities of simulated circuits with Orcad-Capture-PSpice® software. Then, limitations stemming from both the amplifier and the loudspeaker may be clearly identified and separately investigated, while taking account of the nonlinear effects due to the association. Aside from enhancing the amplifier design, this new approach allows us to validate a loudspeaker behaviour both mechanically and electrically closer to reality than any model based on RLC elements. Moreover classical voltage-control can be easily compared with new designs involving current-driving of loudspeakers.

2. Natural specific behaviour of a nonlinear micro-speaker matched with an ideal amplifier

At first, in terms of models, the behaviour of an ideal amplifier fitted with a given loudspeaker is assessed to highlight the nonlinear effects specifically due to the transducer. The latter is implemented as a Simulink® model taking account of all its relevant parameters. As an ideal device, the amplifier is considered as devoid of current and output voltage swing limitations, and with infinite slew rate and bandwidth values. Moreover as regard the integrity of the input signal, bias currents and input offset voltage are equal to zero with an infinite input impedance value. Then, any detected nonlinearity exclusively stems from the loudspeaker. Such a way to proceed will allow hereafter to compare simulation results considering the real data associated with a given amplifier.

2.1. The Thiele and Small lumped parameters model for a given loudspeaker

According to the classical Thiele and Small lumped parameters model (Thiele, 1978), the two differential equations describing a generic loudspeaker behaviour can be written as:

$$u(t) = R_e i(t) + L_e \frac{\mathrm{d}i}{\mathrm{d}t} + Bl\frac{\mathrm{d}x}{\mathrm{d}t}, \tag{1}$$

$$Bli(t) + F_r = M_{ms}\frac{\mathrm{d}^2x}{\mathrm{d}t^2} + R_{ms}\frac{\mathrm{d}x}{\mathrm{d}t} + Kx(t), \tag{2}$$

where $i(t)$ is the coil current [A], $u(t)$ the input voltage [V], $x(t)$ the coil position [m], and the lumped parameters respectively defined with: R_e – voice coil electrical resistance [Ω], L_e – voice coil inductance [H], Bl – force factor [T·m], F_r – Extraneous reluctance force [N], M_{ms} – equivalent mass of the moving voice coil [kg], R_{ms} – mechanical damping parameter and drag force [N·s·m^{-1}], K – suspension stiffness [N·m^{-1}] ($K = 1/C$, C – Compliance [m·N^{-1}]).

An ideal configuration for a loudspeaker should show off invariant parameters. As a matter of fact, technological contingencies cannot allow such a theoretical system, and the real behaviour of a given structure duly have to take account of the significant changes of the lumped parameters against the displacement. This most important point highlights the main interest to develop real time evolutive models. To this end, we consider the specific parameters of a state of the art micro transducer developed by national Panasonic® and commercialized since 2007. As the experimental characterization of its main parameters dependence on the displacement has ever been described in the literature (Strurtzer *et al.*, 2012) we complete the assessment with apt representative fittings so as to achieve a comprehensive Simulink® model. Moreover another shortcoming can be dealt with as regards the extraneous reluctance force that is added in left member of Eq. (2).

2.2. Measured electromechanical parameters changes versus displacement and relevant fittings

The loudspeaker experimented with features a generic 32 Ω internal impedance and a range of displacement values given within the interval [−0.3 mm .. + 0.3 mm]. Then, the measured nominal parameters values, defined at the rest position ($x = 0$), are summed up in Table 1.

Table 1. Nominal electromechanical parameters for a state of the art micro-speaker ($x = 0$).

Parameters	Unit	Value
R_e	Ω	31.75
M_s	g	0.008
K	N/m	41.75
Bl	T·m	0.23
L_e	H	0.06×10^{-3}
R_{ms}	N·s/m	0.009

As regards classical voltage-driving of such a transducer the electrical behavior is depicted in Fig. 1 by way of plotting the impedance changes against frequency considering infinitesimal signals.

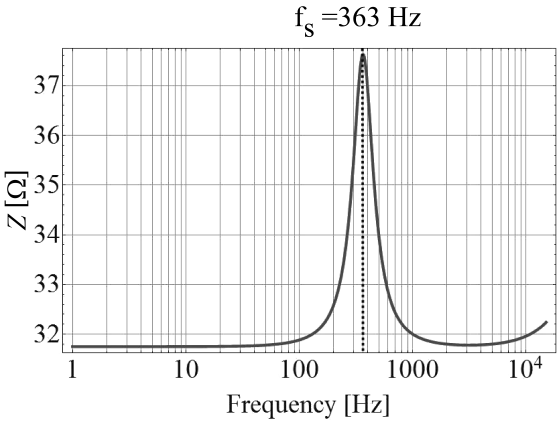

Fig. 1. Impedance of the loudspeaker *versus* the frequency (nominal parameters).

The resonance frequency may be also highlighted while plotting the diaphragm acceleration values against frequency as depicted in Fig. 2, considering relevant conditions as described hereafter (Subsec. 4.4).

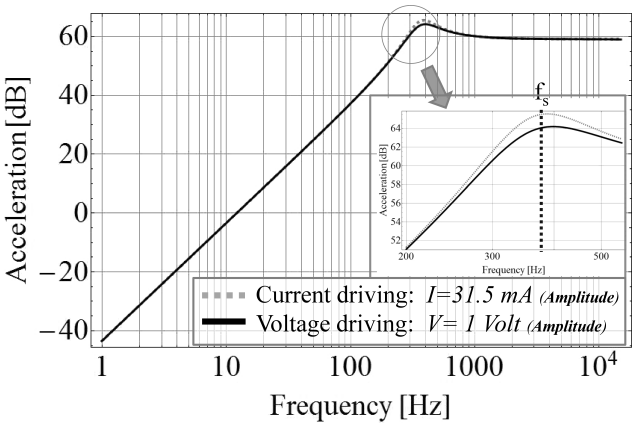

Fig. 2. Acceleration frequency response.

As a loudspeaker nonlinearities mostly stem from its parameters changes with the displacement (Ravaud *et al.*, 2010; Klippel, 1990), relevant measurements formerly carried out proved the importance of such changes, considering the force factor Bl, the stiffness K (respectively C the compliance), and the coil inductance L_e (Klippel, 2001; 2006; Ravaud *et al.*, 2009; Voishvillo *et al.*, 2004; Merit *et al.*, 2004; Kaizer, 1987; Dobrucki, 1988). The values of the three latter parameters are most significantly altered as depicted in Fig. 3, 4, 5 and 6, considering the generic range of displacement values and the effective one [−0.126 mm .. 0.126 mm].

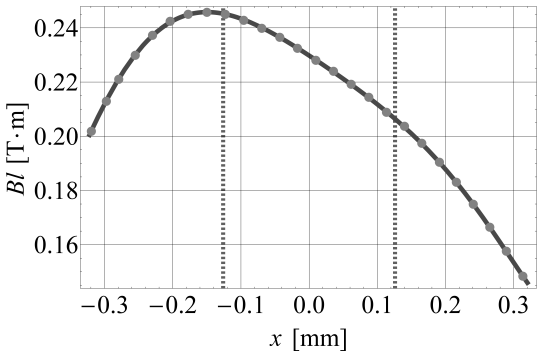

Fig. 3. Force factor Bl against displacement x.

To model such parameters changes against displacement, straightforward polynomial functions can be considered as follows with their appropriate coefficients calculated with standard Matlab® utilities (Curve Fitting Toolbox):

$$Bl(x) = Bl_0 + \sum_{n=1}^{n=p}(Bl_n x^n), \quad (R^2_{Bl} = 1 - 10^{-10}), \quad (3)$$

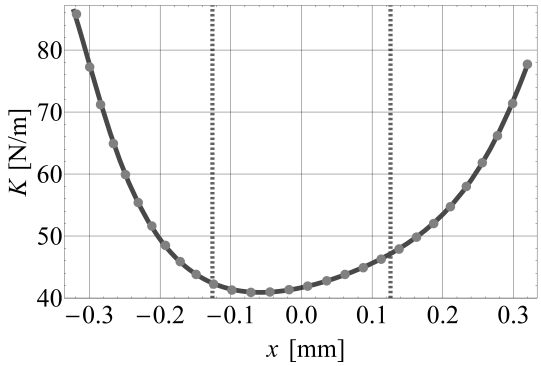

Fig. 4. Stiffness K against displacement x.

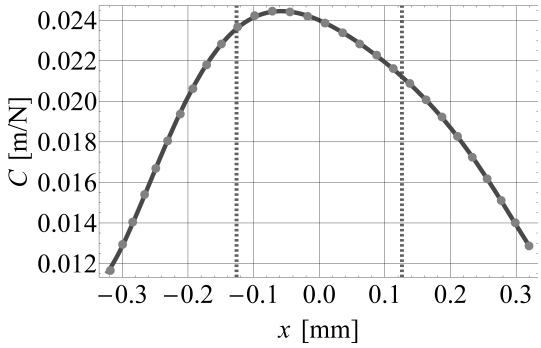

Fig. 5. Compliance C against displacement x.

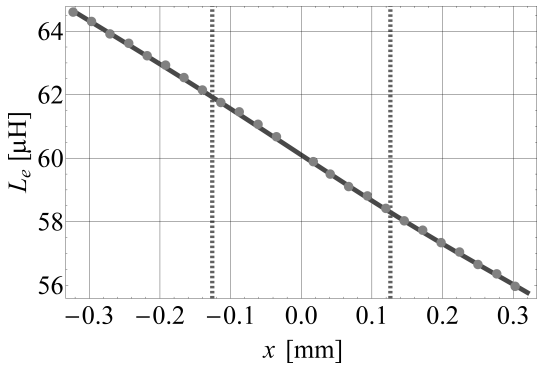

Fig. 6. Coil inductance L_e against displacement x.

$$K(x) = K_0 + \sum_{n=1}^{n=p}(K_n x^n),$$
$$C(x) = K(x)^{-1} = C_0 + \sum_{n=1}^{n=p}(C_n x^n), \quad (4)$$
$$(R^2_K = R^2_C = 1 - 10^{-5}),$$

$$L_e(x) = L_{e_0} + \sum_{n=1}^{n=p}(L_{e_n} x^n), \quad (R^2_{L_e} = 1 - 2.10^{-5}). \quad (5)$$

Both sets of measured values and fitted ones are superimposed in Fig. 3, 4, 5 and 6, relative to the nonlinearities stemming from any displacement. In Table 2 the first six successive estimates for each set of averaged parameters are tabulated for Bl, C (respectively K), and L_e.

Table 2. Polynomial coefficient values for Eq. (3), (4) and (5).

i	Bl_i	C_i	K_i	L_{e_i}
0	0.23	2.4×10^{-2}	41.75	6.01×10^{-5}
1	-1.65×10^{2}	-14.07	25.02	-1.46×10^{-2}
2	-1.61×10^{5}	-8.87×10^{4}	150.37	0.61
3	6.49×10^{8}	3.22×10^{8}	-388.08	1.31×10^{4}
4	-5.97×10^{12}	-8.62×10^{11}	2382.67	6.52×10^{6}
5	1.06×10^{15}	-1.63×10^{15}	74.63	-5.18×10^{10}
6	2.14×10^{19}	5.97×10^{18}	128.09	-4.42×10^{13}

The relevance of the rationale is ensured as the plotted values of both measured and fitted sets prove to be in perfect agreement.

2.3. Simulink® nonlinear models for the micro speaker

Simulink® is a block diagram environment for multidomain simulation and Model-Based Design. It supports system-level design, simulation, automatic code and continuous test. Then, by way of expanding the classical Thiele and Small approach, real time evolutive models can be developed either for voltage or current-driving. Indeed as the representative equations depend both on time and displacement, a relevant numerical solver can take into account all the involved parameters. The whole set of physical quantities, such as displacement, acceleration, current and voltage (in case of current-driving) and so on can be advantageously modeled. Then, the abovementioned polynomial functions allowing for the nonlinear behaviour can be coupled with articulate function blocks enabling us to fit with the evolutive parameters $[Bl(x), K(x), L_e(x)]$. As depicted in Fig. 7 and 8, the model relies on processing the running displacement $x(t)$ as a feedback data for computing in real time each parameter. Considering at the first the classical voltage-controlling, both Eq. (1) and (2) are involved in the model, with voltage as input signal yielding current value prior to acceleration and displacement as output signals taking into account of the reluctance as precised hearafter.

On the other hand considering current-driving Eq. (2) is processed allowing us to get any evolutive parameter. The optional voltage block can be desactivated as needed by the user, as shown in Fig. 7.

2.4. The two-tone stimulus method yielding both electrical and acoustical behaviours

As clearly seen in Fig. 7 and 8 a current-controlling policy is more natural and easy to implement with Simulink®. Then in the following Subsec. 2.4.1. to 2.4.4. only the classical voltage-drive policy is highlighted before assessing both approaches with their driving circuitry. In order to assess the respective impact of any given parameter change, each relative polynomial function can be separately investigated. To this end the parameters variations can be introduced one by one in the Simulink® model. Nonlinear effects can be presented either as entailing harmonic and intermodulation waves generation as regards the electrical

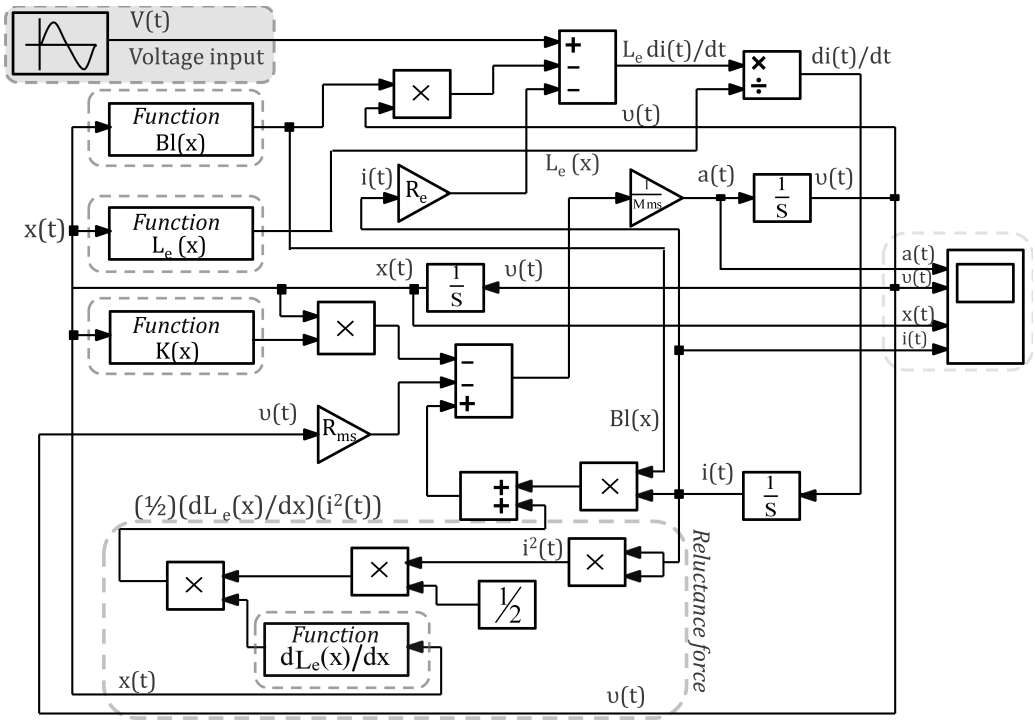

Fig. 7. Simulink® nonlinear recursive model for a given loudspeaker with voltage-driving.

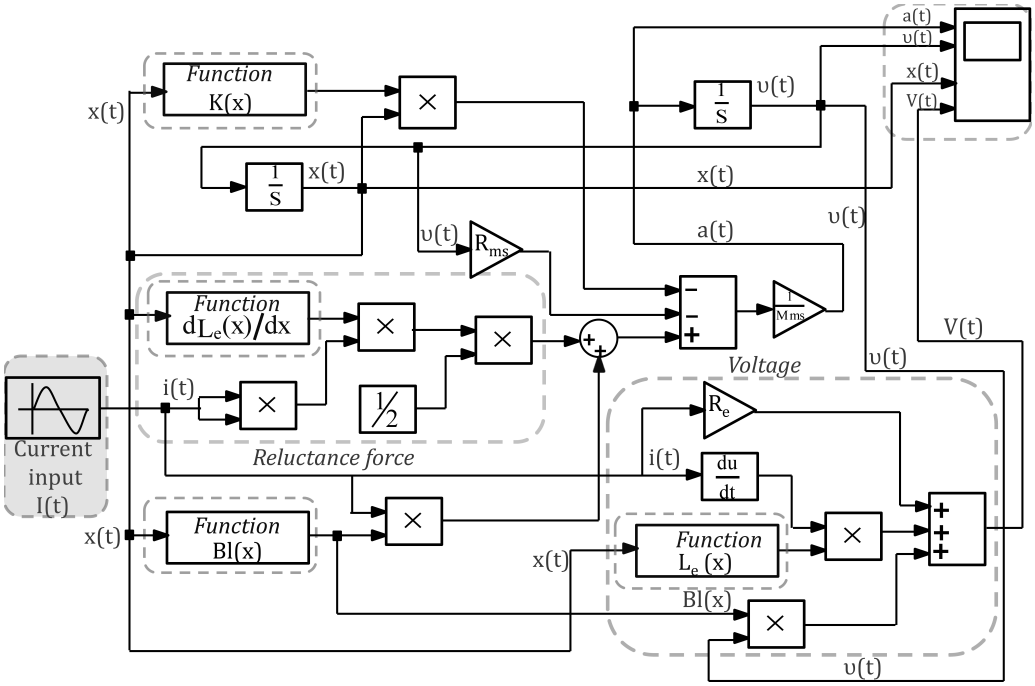

Fig. 8. Simulink® nonlinear evolutive model for a given loudspeaker with current-driving.

current driving the loudspeaker, or with the acceleration inferred from the second derivative of the displacement $x(t)$. Indeed, the latter parameter is closely associated with the sound pressure level issued from the loudspeaker with a straightforward proportionality. Then, for a given simulation both electrical current and related acceleration distortions can be investigated and compared with a view to simplifying the comprehensive analysis of a given loudspeaker. Indeed, if a clear redundancy would appear between current and acceleration, one would obviously prefer to deal with standard electrical measurements rather than undertaking acoustical characterisations involving an expensive anechoic room.

As a matter of fact, our simulation will highlight the lack of redundancy between current and acceleration, thanks to the two-tone stimulus approach together with our Simulink® model. At first, the so-called two-tone driving signal is constructed with two straightforward sinusoïdal components such as:

$$V_{\text{in}} = V_1 \sin(2\pi f_1 t) + V_2 \sin(2\pi f_2 t). \tag{6}$$

The choice of both involved amplitudes should be best suited for the technological structure of the loudspeaker and values have been separately experimented with a view to keeping a RMS current value averaging 20 mA (with 32 Ω). Conversely, both frequencies values, although compatible with the bandwidth of any standard system, are chosen far enough from each other to discriminate the entailed nonlinear effects due to each component. Then the signal is constructed with values given in Table 3. In this rationale

Table 3. Values for the two-tone stimulus signal parameters.

Parameters	Unit	Values
V_1	V	0.944
V_2	V	0.237
f_1	Hz	541
f_2	Hz	5447

$V_{\text{in}} = V(t)$ has to be considered as stemming from an ideal voltage supply ($u_{\text{RMS}} = 0.684$ V), also referred to as a Thevenin source (internal impedance as a short circuit).

As enabled with the structure depicted in Fig. 7, the input signal $V_{\text{in}} = V(t)$ resulting from Eq. (6) (according to two "*Sine Waves*") is processed with the Simulink® model, yielding both electrical current an acceleration values against time. Such behaviours are simulated prior classical treatment with a Fast Fourier Transform. The 0 dB reference line level being that of the fundamental (V_1), then, both fundamental spectral lines can be highlighted together with their respective sets of harmonics due to nonlinear distortions and intermodulations. As a main advantage, both harmonic and intermodulation lines can be investigated in a single simulation process.

2.4.1. Nonlinear distortions due to the Bl(x) Force factor changes

Considering a generic electrodynamic loudspeaker, the force factor stands for the coupling between both

electrical and mechanical properties as regards the Thiele and Small parameters model. As a most important source of nonlinearities the force factor is significantly altered with changing displacement values as highlighted with Fig. 3. It clearly appears that the polynomial function derived from Eq. (3) and Table 2 allows an exact fitting for a relevant behaviour description. This function [in T·m or N·A^{-1}] is written as,

$$\begin{aligned} Bl(x) = {} & 0.23 - 165x - 1.61 \times 10^5 \times x^2 \\ & + 6.49 \times 10^8 \times x^3 - 5.97 \times 10^{12} \times x^4 \\ & + 1.06 \times 10^{15} \times x^5 + 2.14 \times 10^{19} \times x^6 \end{aligned} \tag{7}$$

prior to natural implementation within the Simulink® model instead of the basic nominal constant values given in Table 1. Here, both stiffness and inductance are considered at their rest position. As a result, the respective curves associated with current and acceleration are significantly altered as is clearly shown after FFT processing. As an illustration, both electrical current and acceleration values are respectively depicted in Fig. 9 and 10. Such consecutive changes feature harmonic and intermodulation spectral lines with harmonics displayed as multiples of the fundamental line ($k.f_1$) and intermodulation lines arranged as ($m \cdots f_2 \pm n \cdots f_1$) around the f_2 line (k, m, n, integers).

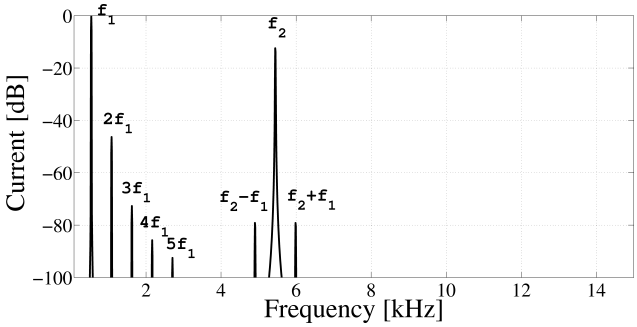

Fig. 9. Extraneous spectral lines as Current distortion due to Force factor changes.

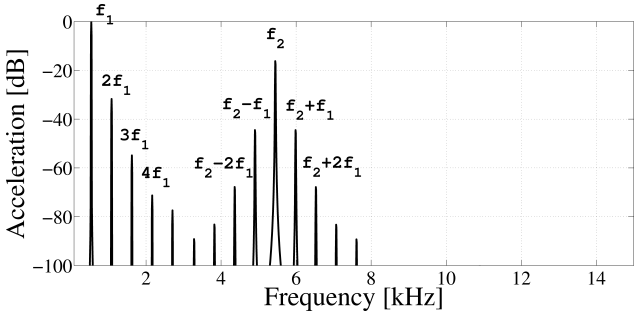

Fig. 10. Extraneous spectral lines as Acceleration distortion due to Force factor changes.

Then, a significant difference between both spectral patterns clearly appears, with harmonics and intermodulations in acceleration quite more marked with acceleration than with current *spectra*. In the literature, a comprehensive experimental approach due to (Klippel, 2006), corroborates the relevance of our model, with intermodulation distortions (IMD) higher for sound pressure level (proportional to acceleration) than for the electrical current.

Moreover, considering Fig. 10, distortions related with the acceleration highlight the significant levels of both the second harmonic ($2f_1$) and the first intermodulation ($f_2 \pm f_1$). In a recent paper (Erza *et al.*, 2011), we justified such a behaviour owing to the asymmetrical variation of the force factor pattern observed against displacement as shown in Fig. 3.

2.4.2. Nonlinear distortion due to the $K(x)$ Stiffness changes

A speaker cone, or diaphragm is technically the cone shaped part, also referred to as the cone/surround assembly to include the outer suspension called the surround. If properly designed in terms of mass, stiffness, and damping, the diaphragm allows to centre and adjust the coil within the magnetic gap, enabling then any expected displacement of the moving voice coil. The purpose of the cone/surround assembly is to accurately reproduce the voice coil signal waveform. Inaccurate reproduction of the voice coil signal results in acoustical distortion. Then, as clearly shown in Fig. 4 and 5, both stiffness and compliance changes associated with any given significant displacement ($x \neq 0$) are a major source of nonlinear distortion. According to Eq. (4) and Table 2, either compliance or stiffness may be respectively written as,

$$\begin{aligned} C(x) = {} & K^{-1}(x) = 2.4 \times 10^{-2} - 14.07 \times x \\ & - 8.87 \times 10^5 \times x^2 + 3.22 \times 10^8 \times x^3 \\ & - 8.62 \times 10^{11} \times x^4 - 1.63 \times 10^{15} \times x^5 \\ & + 5.97 \times 10^{18} \times x^6, \end{aligned} \tag{8}$$

$$\begin{aligned} K(x) = {} & 41.75 + 25.02 \times x + 150.37 \times x^2 \\ & + - 388.08 \times x^3 2382.67 \times x^4 \\ & + 74.63 \times x^5 + 128.09 \times x^6 \end{aligned} \tag{9}$$

before being implemented in the Simulink® model according to the two-tone stimulus input signal. Here, both force factor and inductance are considered at their rest position ($x = 0$). After FFT processing, the respective curves associated with current and acceleration can be plotted as depicted in Figs. 11 and 12. Then, as regards electrical current, it is clear from Fig. 11 that stiffness changes do not bring out any intermodulation spectral lines. Figure 12, relative to the acceleration behaviour, highlights intermodulaion lines together with harmonics quite more delineated (about 26 dB for each one) than with the current behaviour. Hence, as regards stiffness changes it can be concluded that the loudspeaker distortion is essentially due to the occurrence of harmonic distortion, with intermodulation extraneous lines remaining almost insignificant.

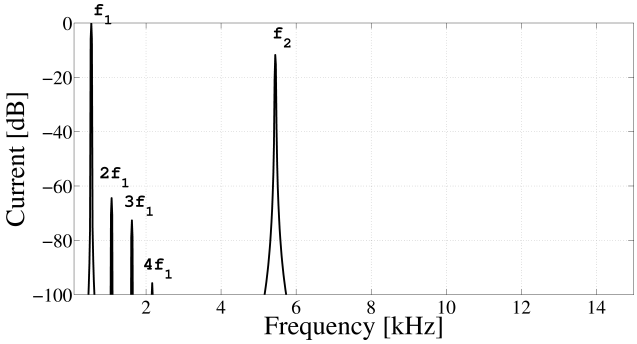

Fig. 11. Extraneous spectral lines as Current distortion due to Stiffness changes.

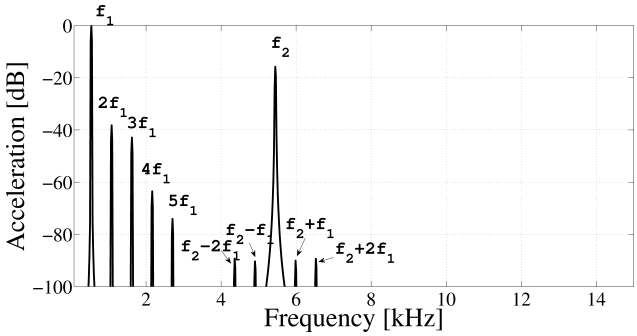

Fig. 12. Extraneous spectral lines as Acceleration distortion due to Stiffness changes.

Here, signals are less impaired as regard second harmonic than with the Bl force factor changes.

2.4.3. Nonlinear distortion due to the $L_e(x)$ Inductance changes yielding a Reluctance force

Two nonlinear effects result from inductance changes. Aside from the first, stemming from the change of its own, a nonlinear term referred to as a reluctance force $\{i^2 d(L_e(x))/dx\}$ is introduced in the differential formulation (Erza *et al.*, 2012). Such an extraneous force depends both on the inductance change observed with the displacement, and also on the current squared value. Then the mechanical behaviour featured with Eq. (2) can be expressed as:

$$Bli(t) + \frac{1}{2}\frac{\mathrm{d}L_e(x)}{\mathrm{d}x}i^2 = M_{ms}\frac{\mathrm{d}^2x}{\mathrm{d}t^2} + R_{ms}\frac{\mathrm{d}x}{\mathrm{d}t} + Kx(t). \quad (10)$$

Considering both Eq. (5) and Table 2, the influence of any inductance change against the displacement can be fitted with:

$$\begin{aligned} L_e(x) = {} & 6.01\times10^{-5} - 1.46\times10^{-2}\times x \\ & + 0.61\times x^2 + 1.31\times10^{4}\times x^3 \\ & + 6.52\times10^{6}\times x^4 - 5.18\times10^{10}\times x^5 \\ & - 4.42\times10^{13}\times x^6. \end{aligned} \quad (11)$$

As before, introducing this quantity in the Simulink® model prior FFT processing allows us to plot both current and acceleration spectral patterns as illustrated with Figs. 13 and 14.

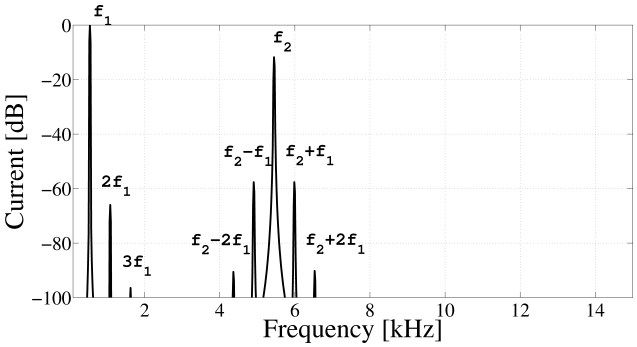

Fig. 13. Electrical current spectral distortion due to inductance changes.

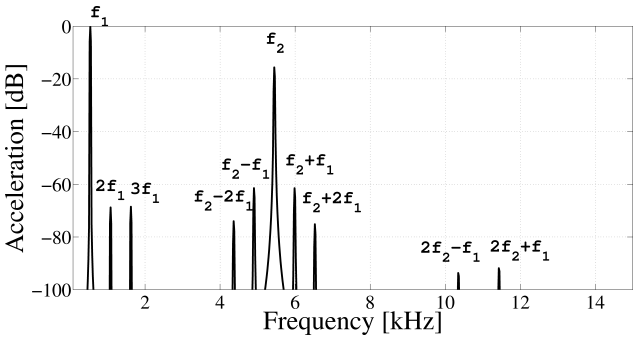

Fig. 14. Acceleration spectral distortion due to inductance changes.

As could be expected from the minor relative changes observed in Fig. 6, the impact as nonlinear distortion regarding both current and acceleration is quite lower than with both previous cases. Considering both current and acceleration *spectra*, second harmonic lines ($2f_1$) and both first intermodulation lines ($f_2 \pm f_1$) show off about the same levels. However, both third harmonic ($3f_1$) and intermodulations ($f_2 \pm 2f_1$) lines are more significant with acceleration than with current behaviours, as justified with the Klippel experimental approach (Klippel, 2006). Then, high frequencies generally introduce an overall distortion as intermodulation lines.

2.4.4. Nonlinear distortion due to the all-inclusive set of changes

The effects of independent changes considered respectively with $Bl(x)$ the Force factor, $K(x)$ the Stiffness and $L_e(x)$ the Inductance have been separately assessed, it is possible now to combine the three influences while implementing Eq. (7), (9) and (11) in the Simulink® model. After FFT processing, the new patterns of spectral lines are respectively depicted in Fig. 15 as regards electrical current, and Fig. 16 dealing with the acceleration behaviour. As could be ex-

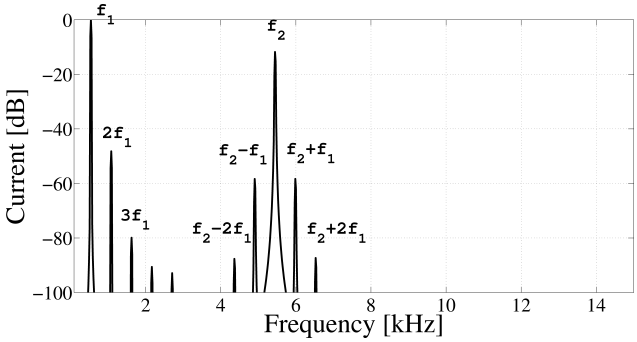

Fig. 15. Electrical current spectral distortion due to the all-inclusive set of changes.

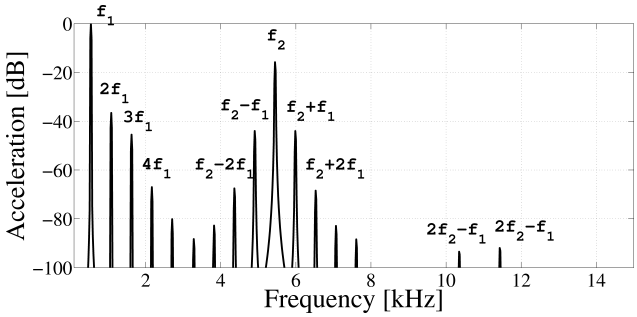

Fig. 16. Acceleration spectral distortion due to the all-inclusive set of changes.

pected from previous independent cases, both figures highlight an overall distortion mostly marked on the acceleration spectral lines with a quite moderate alteration impairing the electrical current spectrum. As a result, it is clear that measurements dealing only with the electrical current are not enough of their own to account for the exact behaviour of a given loudspeaker, insofar as nonlinearities occur due to a significant value of the displacement within its nominal range and that also far beyond 363 Hz the resonance frequency. Then for a comprehensive investigation, electrical measurements can be seen only as a first step that should be completed with acoustical measurements.

3. Shortcomings of a real amplifier and their Influence

Effective sound processing with a given loudspeaker depends both of the latter and its driving amplifier. Until now the simulations dealt with the drawbacks of a given microspeaker considering an ideal amplifier. A real case should consider the technological limitations due to the integrated electronic structure of the amplifier. The following drawbacks may alter significantly the rendering of any musical piece as regards a given imperfect audio line driver:

1. The Input Bias Current (IBC) is unfortunately different from zero, and may reach up to 200 nA.
2. Unbalanced structures may also feature Input Offset Current Values often up to 20 nA.
3. The output impedance differs from zero, values ranging from 1 Ω up to 600 Ω or more, depending on the specific purpose of the device.
4. Stringent nonlinear limitations may appear considering the Gain value and the Output Voltage Swing capabilities of the device, together with possible phase shifts.
5. The Slew Rate (SR)Value, defined as the average time of change of the closed-loop amplifier output voltage for a step signal input, should be infinite. For high quality audio performance its value should exceed SR ≥ 8 V/μs.
6. At last, all noise sources should be minimized and pop-noise eradicated. Considering Equivalent Input Voltage Noise (V_n), values lower than 2 nV/($\sqrt{\text{Hz}}$) should be recommended.

Then, it is of crucial interest to simulate the behaviour of a real audio system combining both the drawbacks of the loudspeaker and its associated amplifier. Considering nonlinearities, such a comprehensive study is mandatory prior to actual implementation with real devices.

4. Linking advanced software, Simulink® for the transducer, and Orcad-Capture-PSpice® for the amplifier

Nowadays, Orcad-Capture-PSpice® is considered as a most powerful software for schematic design solutions in electronics. Most of the linear integrated circuits such as amplifiers can be accurately simulated with, saving time and cost for the designer. At first the amplifier can be loaded with a straightforward resistor, allowing to achieve a comprehensive time domain output analysis (Transients, DC Sweep Wobulation) befor considering a loudspeaker as a nonlinear electromechanical system, with its own specific mechanical parameters.

Since a given transducer cannot be simplified as a linear load, and the abovementioned approaches (Vanderkooy, 1989; Wright, 2008) based on RLC circuits together with Orcade-Capture-PSpice® should prove unable to accurately simulate a relevant real case. Indeed in such models both electrical and mechanical changes against displacement cannot be taken into account, and they are impeded over their first purpose restricted to highlight the impedance *versus* frequency. Then as a most valuable solution we stress the interest to combine Simulink®-based electromechanical models with virtual amplifiers simulated with Orcade-Capture-PSpice®. To this end the advanced SLPS (Simulink-PSpice) co-simulator proves especially suited.

4.1. The SLPS co-simulation environment

An effective co-simulation environment is available with the SLPS utility that allows to combine two advanced simulation tools. Indeed the standard Orcade-Capture-PSpice® electronic environment can be associated with mathematical models of elaborate systems such as an electrodynamic loudspeaker described with Simulink®. This approach allows to deal with executable system-level specifications to design advanced hybrid systems. As regard electronic devices, Orcade-Capture-PSpice® provides realistic models allowing for nonlinearities, delay, and various other drawbacks encountered with real devices. As an advantageous approach, co-simulations make possible system-level interfaces to be tested, taking account of their actual physical properties avoiding then the realization of prototypes. As a result design issues may be quickly dealt with, saving both cost and time considering the tedious issue of debugging the trail boards of system prototypes.

4.2. Implementing Simulink® speaker models with a PSpice® amplifier model

The SPLS co-simulator relies on block diagrams enabling to assemble simulated electronic devices with the abovementioned nonlinear model of a loudspeaker. The electrical parameters of the amplifier are defined with PSpice® prior SLPS implementation as a block in the specific Simulink® environment as depicted in Fig. 17.

Either voltage or current values can be sampled prior to interfacing with SLPS blocks.

As regards the amplifier block, both input and output accesses can be conveniently arranged as required by the designer to connect any kind of device defined as other relevant blocks as highlighted in Fig. 17 for our specific purpose.

On the left, the electrical circuitry consists of a straightforward closed-loop amplifier together with a conditioning box (ZX) acting as a lonlinear conecting load whose value is actuated with a driving voltage (V_{ref}). Such a block behaves as an externally controlled resistor with:

$$Z_{\mathrm{out}} = R_{\mathrm{base}} \times (V_{\mathrm{ref}}/V_0) \quad \text{with } V_{\mathrm{ref}} \text{ Control voltage,}$$
$$R_{\mathrm{base}} = 1\Omega, \quad \text{and} \quad V_0 = 1V. \tag{12}$$

On the top of Fig. 17 a first approach is given with a classical voltage-driving design. Then, the PSpice® non ideal amplifier is arranged with the loudspeaker simulink® model as a whole nonlinear hybrid system. Numerical values are computed with a sampling frequency allowing 2048 samples for the period of the fundamental of the input signal. As highlighted in Fig. 17 a nonlinear specific test load can be assessed (S_2 on, S_1 off) while operating the S_1/S_2 selector befor implementing the trancducer as defined with Fig. 7 (S_2 disabled, S_1 on). On the other hand, current-driving of the transducer is depicted with SLPS2 block as illustrated in the bottom of Fig. 17, allowing

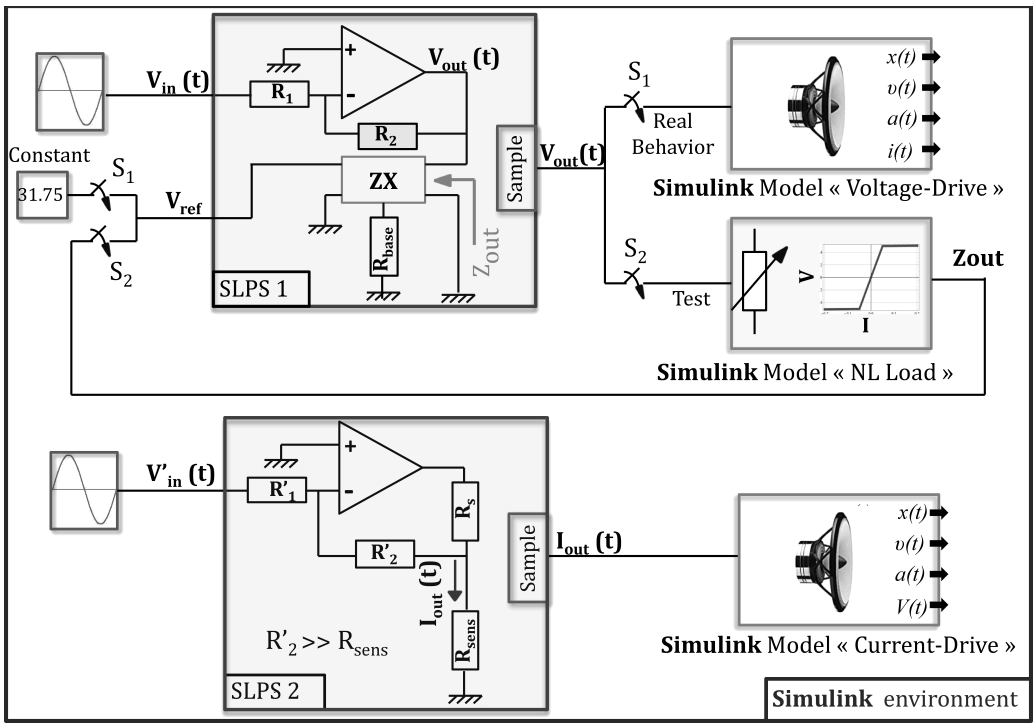

Fig. 17. Simulink block diagram of the model of nonlinear loudspeakers supplied with imperfect amplifiers.

to V'_{in} as a driving voltage into its associated proportional current feeding the loudspeaker as defined with Fig. 8.

The relevance of the approach is confirmed after checking the right implementation of the simulink model. To this end the behavior of the so so-called NL Load is assessed considering the following relationships linking electrical quantities :

$$\begin{aligned} &Z_{\text{out}} = 10\ K\Omega \quad \text{if} \quad -0.5V \leq V_{\text{out}} \leq 0.5V, \\ &Z_{\text{out}} = 32\ \Omega \qquad \text{if} \quad V_{\text{out}} < -0.5V \ \text{ or } \ V_{\text{out}} > 0.5. \end{aligned} \tag{13}$$

Then this load supplied with the following sinusoidal voltage:

$$V_{\text{in}} = V_1 \sin(2\pi f t) \quad \text{with} \quad V_1 = 1\ \text{Volt}_{\text{RMS}} \quad \text{and} \quad f = 540\ \text{Hz}. \tag{14}$$

As a result, considering a unity gain ($R_1 = R_2 = k\Omega$) with a classical LM741 amplifier, the ZX corrector allows a current behavior as depicted in Fig. 18.

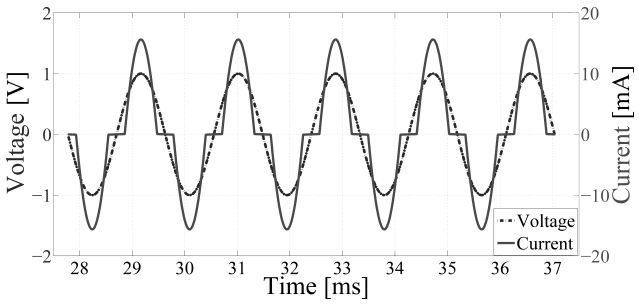

Fig. 18. Current behavior due to the nonlinear load.

After such a checking process the transducer can be implemented and assessed on its own (S_1 on, S_2 off), the corrector ZX being driven with the constant voltage set value $V_{\text{ref}} = 31.75$ V.

4.3. Acceleration behaviour with a real amplifier compounded with the micro speaker

Considering both voltage and current-driving schemes the two-tone stimulus method as described in 2.4. can be used to investigate with the whole emulated system involving both a non ideal amplifier together with a nonlinear loudspeaker. Then different amplifiers can be compared as regards a given transducer by way of computing the distortion of its acceleration parameter as regards the moving diaphragm: as a result, such a study allows us to choose at best among several prospective amplifier units or driving schemes when comparing their respective distortion patterns.

4.3.1. Respective nonlinear effects for two different amplifiers

In order to highlight the interest of the approach two kinds of amplifiers far different from one another are considered. At first, a general purpose unit is implemented with the standard characteristics of the generic LM 741 (T.I®). Among its most salient parameters (IBC = 30 nA), such a device features a poor slew rate value with SR = 0.5 V/µs at unity gain, and a fair noise capability with $V_n \approx 50\ \text{nV}/\sqrt{\text{Hz}}$ around $f = 100$ Hz. The output resistance is 75 Ω with a maximum allowable current up to 25 mA. Considering the 32 Ω transducer supplied with the RMS voltage value ($u_{\text{RMS}} = 0.684$ V), the associated current (20 mA) with such a regime is significant compared with the overload limit. Conversely, the second chosen reference deals with a power operational amplifier dedicated to audio purposes, the OPA549: The IBC bias current is 100 nA, the slew rate value is given as SR = 9 V/µs, and as regards noise voltage, $V_n \approx 70\ \text{nV}/\sqrt{\text{Hz}}$ around $f = 1000$ Hz. The main difference with the former unit stands with its high output current capability up to 8 A. Here, the device is (at the opposite) far from its overload regime.

Considering both amplifiers associated with the nonlinear Simulink® model of the transducer in the voltage-driving scheme, the entailed acceleration distortion *spectra* are respectively depicted in Fig. 19 and 20. In both cases, the components are considered as supplied with standard voltage values [$V_{cc-} = -12$ V, $V_{cc+} = +12$ V]. It is clear that the coupling with the general purpose unit (LM741) is fitted with more distortion than the association audio amplifier (OPA 549) and micro speaker. Both compounds com-

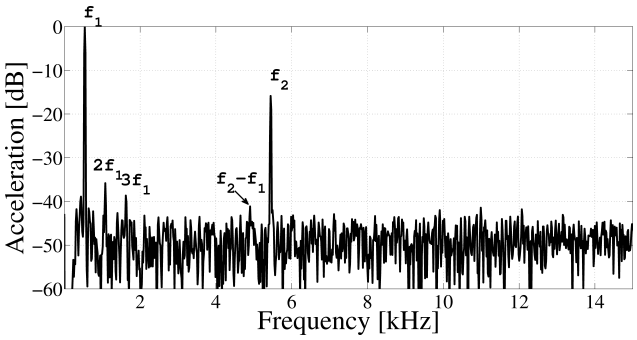

Fig. 19. Acceleration spectrum of micro speaker fed with LM741.

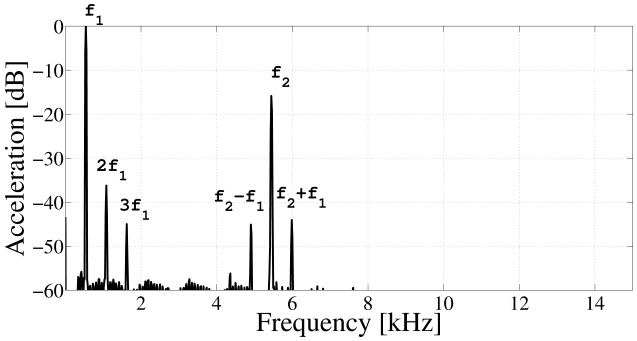

Fig. 20. Acceleration spectrum of microspeaker supplied by OPA549.

pared with one another prove the OPA 549 almost noiseless. Moreover, considering Fig. 19 compared with Fig. 16, the third harmonic line ($3f_1$) is significantly increased (almost +6 dB) highlighting a salient shortcoming for the 741 unit. Conversely with the OPA 549 audio device, this effect is far less stressed, with less than +3 dB.

Then, as expected the general purpose amplifier is far less instrumental than the audio one. Indeed such a device is fitted for low cost appliances, for instance radio alarm clocks. Hence, our approach enables to investigate on the acoustic quality with regards to cost for any given audio system.

4.3.2. Influence of the gain value

Considering a given amplifier with a classical voltage-driving scheme, designers and manufacturers provide spectral noise density values as an input signal. Then the output noise depends directly on the closed-loop gain value according to the selected configuration, either inverting or non-inverting. Indeed, increasing the gain yields more noise. As shown in Fig. 17 (Voltage scheme) the gain of the straightforward inverting structure ($G = -R_2/R_1$) can be modified while changing R_2 and keeping $R_1 = 1$ kΩ.

In this section simulations are now considered with the OPA 549 audio device and carried out while keeping constant the output voltage of the amplifier. Respective gain values are chosen as, $G = 1$, $G = 100$, $G = 300$, so as to compare the nonlinear effects associated with noise and total harmonic distortion. The output voltage is defined as a simple sinusoidal signal with:

$$V_{\text{out}} = V_1 \sin(2\pi f t) \quad \text{with} \quad V_1 = 1 \text{ Volt}_{\text{RMS}} \quad \text{and} \quad f = 540 \text{ Hz}. \tag{15}$$

Such a signal drives the Simulink® loudspeaker model according to the three considered gain values. Then as depicted in Fig. 21, 22 and 23, the acceleration *spectra* can be compared, clearly highlighting how the signal is impaired as the gain is increased as seen in Table 4.

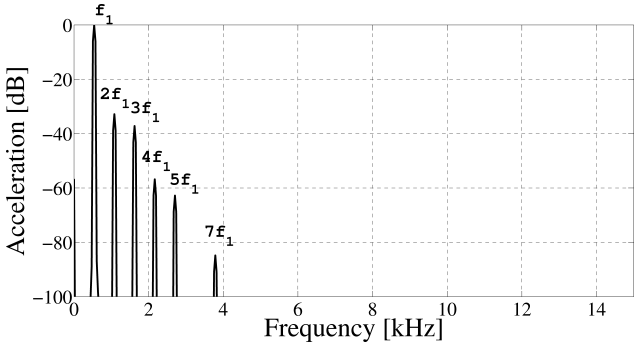

Fig. 21. Acceleration spectrum of microspeaker supplied by OPA549 gain = 1.

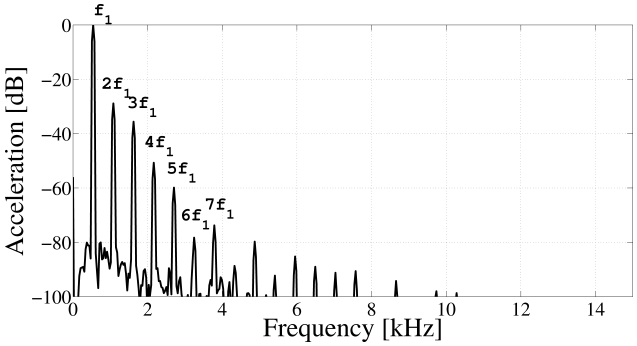

Fig. 22. Acceleration spectrum of microspeaker supplied by OPA549 gain = 100.

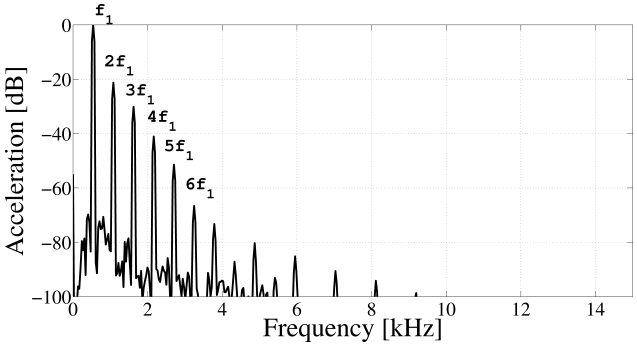

Fig. 23. Acceleration spectrum of microspeaker supplied by OPA549 gain = 300.

Table 4. Harmonic spectrals and THD mesurements when the gain varies by 1, 100 and 300.

Spectral line [dB]	$G = 1$	$G = 100$	$G = 300$
$2f_1$	−32.84	−28.87	−21.28
$3f_1$	−37.2	−35.61	−30.16
$4f_1$	−56.81	−50.72	−41.08
$5f_1$	−62.8	−59.88	−51.45
$6f_1$	negligible	−78.29	−66.63
$7f_1$	−84.84	−73.77	−73.28
THD%	3.88	5.68	12.95

As a result it is clear that Total Harmonic Distortion is most significantly increased as the amplifier gain is increased.

4.4. A brief comparison between voltage and current driving schemes

Although voltage-controlling of transducer is the most common policy abided to by designers and manufacturers, the natural physical quantity acting for moving the voice-coil is the current, then directly assosiated with the acceleration and entailed sound pressur level.

Voltage is only a secondary quantity mostly flowed with the impedance behavior in case of voltage-driving scheme. Hence distortion should be signifi-

cantly reduced with ideal current-driving associations (Meriläinen, 2009; Gaviot *et al.*, 2014). For the propose of omparision, the choosen amplifier is a high-quality unit, LMH6622 (T.I®) fitted most advantageous characteristics. Indeed, with a low noise $V_n \approx 20\ \mathrm{nV}/\sqrt{\mathrm{Hz}}$ and most enhanced SR = 85 V/µs, such a device shown an output current capability up to 90 mA covering then largely the transducer requirement with a low output resistance ($R_{\mathrm{out}} < 0.1\ \Omega$ at 1 kHz).

Then as regard both voltage and current schemes, a gain value $G = 3$ is considered with a view to maintaining stability as recommended by the manufacturer. A bitone stimulus signal, with a 30 mW power (close to that allowed by the transducer), is defined as summerized in Table 5 with current values infered from voltage and the nominal resistance of the transducer. The purpose of this high power value is to stress the effects of increased displacement values highlighting then the nonlinear distortion. The bitone current signal is defined with:

$$I_{\mathrm{out}} = I_1 \sin(2\pi f_1 t) + I_2 \sin(2\pi f_2 t). \tag{16}$$

Table 5. Values for the two-tone stimulus signal parameters to meet a 30 mW power value.

Parameters	Unit	Values
V_1	V	0.98
V_2	V	0.98
I_1	A	30.5
I_2	A	30.5
f_1	Hz	541
f_2	Hz	5447

Results of the comparison dealing with accelerations are shown in Fig. 24 and 25 with a zero dB reference assosiated with a 0 dB SPL considering the acceleration. On both schemes fundamental levels are kept invariant then fitted with identical sound power.

However second intermodulation lines ($f_2 \pm 2f_1$) stay below 0 dB for the current-driving scheme wherever voltage-driving is flowed with 6.79 dB ($f_2 - 2f_1$) and 5.11 dB ($f_2 + 2f_1$).

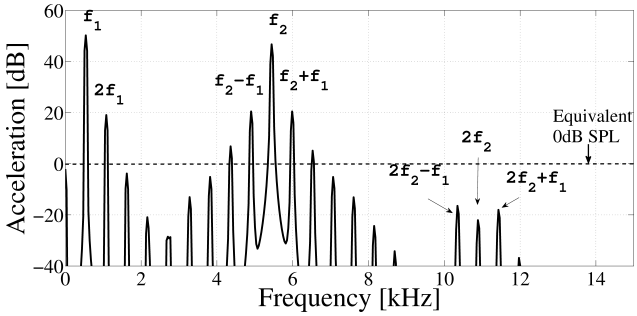

Fig. 24. Acceleration spectral distortion due to the voltage-driving.

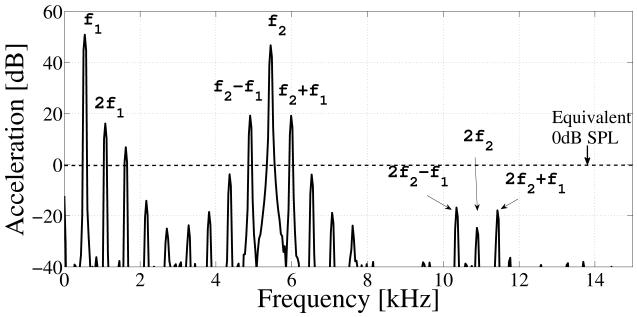

Fig. 25. Acceleration spectral distortion due to the current-driving.

Table 6 summarizes the effective values associated with both driving schemes considering the audible SPL range (level > 0). Then with THD% and IMD% values to be compared, the advantages of current driving are clearly highlighted.

Table 6. Audible distortion for the purpose of comparison between voltage and current-driving.

Spectrals	Voltage-drive	Current-drive
f_1	50.21	50.85
f_2	46.71	46.71
$2f_1$	19.3	16.1
$3f_1$	−3.82	6.81
$f_2 - f_1$	20.45	19.16
$f_2 + f_1$	20.46	19.14
THD%	3.110	2.547
IMD%	8.322	5.759

As a further study we shall investigate on the most relevant approach regarding the analysis of Transient Intermodulation Distortion (TIM), given in (Leinonen *et al.*, 1977). In this way, a square wave (3.18 kHz) and a sinusoid (15 kHz) with a peak to peak ratio of 4:1 are compounded so as to entail valuable information on delays due to the feedback loop.

5. Conclusion

In this paper, the nonlinear effects observed in loudspeakers are investigated with a view to understanding the respective influences of the shortcomings of the main descriptive parameters. As nominal values of the latter (Force factor, Stiffness, Coil inductance) are significantly altered with changes of the voice coil displacement, our Simulink® model allows us to consider separate influences together with the coupling of said changes mostly in terms of respective acceleration *spectra*. Considering a whole audio system, the previous approach is completed by way of compounding the Simulink® behaviour with that of given PSpice® amplifier models. The influence of two distinctive ampli-

fiers is assessed, establishing clearly the advantage of the audio purpose unit. Then, behaviour comparisons are drawn considering different gain values with respectively $G = 1$, $G = 100$, $G = 300$. Once it becomes clear that the nonlinear alteration rises dramatically as the gain is increased, we highlight the interest about driving the transducer with a current regime. Then, as regard distortion within acceleration *spectra*, the latter proves a most advantageous approach to enhancing the amplifier and transducer matching yielding then the best audio quality. It is expected that integrating current driven devices with micro transducers will soon be considered a most valuable manufacturing policy.

References

1. Dobrucki A. (1988), *Constant component of the loudspeaker diaphragm displacement caused by nonlinearities*, 84th AES convention, Number 2577, Paris, France.
2. Erza M., Lemarquand G., Lemarquand V. (2011), *Distortion in Electrodynamic Loudspeaker Caused by Force Factor Variations*, Archives of Acoustics, **36**, 4, 873–885.
3. Erza M., Lemarquand G., Lemarquand V. (2012), *Contribution of the reluctance force to the signal distortion in electrodynamic loudspeakers*, IEEE International Magnetics Conference Intermag, Vancouver, Canada.
4. Gaviot E., Erza M., Polet F., Camberlein L., Bûche B. (2014), *A Versatile Analytical Approach for Assessing Harmonic Distortion in Current-Driven Electrodynamic Loudspeakers*, Journal of Audio Engineering Society, **62**, 3, 127–144.
5. Kaizer AJM. (1987), *Modeling of the nonlinear response of an electrodynamic loudspeaker by a Volterra series expansion*, Journal of Audio Engineering Society, **35**, 421–433.
6. Klippel W. (1990), *Dynamic measurement and interpretation of nonlinear parameters of electrodynamic loudspeakers*, Journal of Audio Engineering Society, **38**, 944–955.
7. Klippel W. (2001), *Speaker auralisation subjective evaluation of nonlinear distortion*, 110th AES Convention, Amesterdam, The Netherlands.
8. Klippel W. (2004), *Nonlinear Modeling of the Heat Transfer in Loudspeakers*, Journal of Audio Engineering Society, **52**, 1/2, 3–25.
9. Klippel W. (2006), *Loudspeaker nonlinearities – cause, parameters, symptoms*, Journal of Audio Engineering Society, **54**, 907–939.
10. Leinonen E., Otala M., Curl J. (1977), *A Method for Measuring Transient Intermodulation Distortion (TIM)*, Journal of Audio Engineering Society, **25**, 4, 170–177.
11. Meriläinen E. (2009), *Current-driving of Loudspeakers*, CreateSpace Independent Publishing Platform, USA.
12. Merit B., Lemarquand V., Lemarquand G., Dobrucki A. (2009), *Motor nonlinearities in electrodynamic loudspeakers: modelling and measurement*, Archives of Acoustics, **34**, 4, 407–418.
13. Mills P.G.L., Hawksford M.O.J. (1989), *Distortion Reduction in Moving-Coil Loudspeaker Systems Using Current-drive technology*, Journal of Audio Engineering Society, **37**, 3, 129–149.
14. Ravaud R., Lemarquand G., Roussel T. (2009), *Time-varying non linear modeling of electrodynamic loudspeakers*, Applied Acoustics, **70**, 3, 450–458.
15. Ravaud R., Lemarquand G., Lemarquand V., Roussel T. (2010), *Ranking of the nonlinearities of electrodynamic loudspeaker*, Archives of Acoustics, 35, 1, 49–66.
16. Sturtzer E., Pillonnet G., Lemarquand G., Abouchi N. (2012), *Comparison between voltage and current driving methods of a micro-speaker*, Applied Accoustics, **73**, 1087–1098.
17. Thiele A.N. (1978), *Loudspeakers in Vented Boxes, Parts 1 and 2*, Journal of Audio Engineering Society, New York.
18. Thorborg K., Unruh A. (2008), *Electrical Equivalent Circuit Model for Dynamic Moving-Coil Transducers Incorporating a Semi-Inductor*, Journal of Audio Engineering Society, **56**, 9, 696–709.
19. Vanderkooy J.R. (1989), *A model of loudspeaker driver impedance incorporating eddy currents in the pole structure*, Journal of Audio Engineering Society, **37**, 119–128.
20. Voishvillo A., Terekhov A., Czerwinski E., Alexandrov S. (2004), *Graphing, interpretation, and comparison of results of loudspeaker nonlinear distortion measurements*, Journal of Audio Engineering Society, **52**, 4, 332–357.
21. Wright J. (2007), *An Emirical Model for Loudspeaker Motor Impedance*, 122th AES Convention, Vienna, Austria.